Electronic supplementary materials *Mendeleev Commun.*, 2023, **33**, 372–375

How electron delocalization influences the electron-withdrawing properties of isomeric benzobischalcogenadiazoles

Elena O. Levina, Ekaterina V. Bartashevich, Alexey E. Batalov, Oleg A. Rakitin and Vladimir G. Tsirelson

Methodology

The fermionic potential v_f, being composed from the exchange, $v_x(\boldsymbol{r})$, and Pauli, $v_P(\boldsymbol{r})$, potentials:

$$v_f(\boldsymbol{r}) = v_x(\boldsymbol{r}) + v_P(\boldsymbol{r}) \quad (1)$$

can be explicitly rewritten in terms of their components.

The exchange potential

$$v_x(\boldsymbol{r}) = \int \frac{h_x(\boldsymbol{r},\ \boldsymbol{r}')}{|\boldsymbol{r} - \boldsymbol{r}'|} d\boldsymbol{r}' + v_x^{resp}(\boldsymbol{r}) \quad (2)$$

consists from the average depth of the Fermi hole weighted by the distance between the points $\boldsymbol{r}$ and $\boldsymbol{r}'$ [1–3] and the static response potential, v_x^{resp}, measuring sensitivity of the exchange correlation hidden in the pair correlation function to electron density variations.[S3–S5] The first v_x component is all over space everywhere, producing stabilizing contribution to the electron energy density, while $v_x^{resp} > 0$ yields small destabilizing effect. Due to the relative smallness of v_x^{resp} [S6], we excluded it from the consideration.

The potential Pauli, v_P, characterizes variability of the Fermi hole in the proximity of point $\boldsymbol{r}$ and the response of the kinetic potential to the local electron density changes.[S3] Using so-called Fermi orbital, $f(\boldsymbol{r},\boldsymbol{r}')$, we can write the Fermi hole as $h_x(\boldsymbol{r},\boldsymbol{r}') = -|f(\boldsymbol{r},\boldsymbol{r}')|^2$ [S7] and arrive at the expression

$$v_P(\boldsymbol{r}) = \frac{1}{2}\int |\nabla_{\boldsymbol{r}} f(\boldsymbol{r},\boldsymbol{r}')|^2\, d\boldsymbol{r}' + v_{kin}^{resp}(\boldsymbol{r}). \quad (3)$$

In other words, first v_P component depends on the rate of change of the Fermi orbital $\nabla_{\boldsymbol{r}} f(\boldsymbol{r},\boldsymbol{r}')$ with changing position of the reference electron at point $\boldsymbol{r}$, while v_{kin}^{resp} measures sensitivity of the exchange correlation hidden in kinetic potential to electron density variations.[S6] Since both of them have destabilizing character, the $v_P > 0$ everywhere in the molecule.

Taking that into account, one can interpret regions with $v_f > 0$ (v_P values dominate over the v_x values) as ones where kinetic component of the exchange correlation is dominated over the static one. In other words, in the vicinity of these regions Fermi hole changes its shape rapidly and, in these regions, also the kinetic potential response to the density variations is high. Therefore, areas with $v_f > 0$ indicate proximity of the areas with rapidly changing electron localization.[S1] On the contrary, $v_f < 0$ indicates areas where static contribution to the electron correlation is dominated (Fermi hole depth prevails all other factors). Therefore, $v_f < 0$ denote regions with highest electron localization.

In the current work we mainly considered full v_f potential. It was computed via the Euler–Lagrange equation for electron density[S6,S8,S9]

$$v_f(\boldsymbol{r}) = \mu + v_{esp}(\boldsymbol{r}) - v_W(\boldsymbol{r}), \tag{S4}$$

where μ is a chemical potential of the system (μ equals energy of the higher occupied molecular orbital),[S8,S10] v_{esp} is an electrostatic potential[11] and v_W is a Weizsäcker potential.[S11–S13] One should note that this expression is defended for systems, computed in the full basis set. Use of the Gaussian functions leads to the v_f unphysical oscillations in the regions close to the atomic nucleuses.[S14] Therefore, we did not discuss these areas in the current study.

To illustrate role of the fermionic potential part dependent only on the Fermi hole depth and Fermi hole's tendency to change $v_f^{hole} = \int \frac{h_x(\boldsymbol{r},\boldsymbol{r}\prime)}{|\boldsymbol{r}-\boldsymbol{r}\prime|} d\boldsymbol{r}' + \frac{1}{2}\int |\nabla_{\boldsymbol{r}} f(\boldsymbol{r},\boldsymbol{r}')|^2 \, d\boldsymbol{r}'$ we extracted from the v_f the kinetic response potential, calculated as[S3]:

$$v_{kin}^{resp}(\boldsymbol{r}) = \mu - \sum_i \varepsilon_i \frac{\varphi_i^2(\boldsymbol{r})}{\rho(\boldsymbol{r})}, \tag{5}$$

(small $v_x^{resp}(\boldsymbol{r})$ contribution to the v_f was ignored). In the eq. (5) ε_i are energies of the occupied molecular orbitals φ_i and $\rho(\boldsymbol{r})$ is an electron density. Note, that the $v_x^{resp}(\boldsymbol{r})$ was excluded from the consideration.

The exchange potential was reduced to its Fermi-hole dependent part (see eq. 2) and the Fermi hole itself was calculated as

$$h_x(\boldsymbol{r},\boldsymbol{r}') = \frac{1}{\rho(\boldsymbol{r})}\left(-\sum_{i=\alpha}\sum_{j=\alpha} \varphi_i^*(\boldsymbol{r})\varphi_j^*(\boldsymbol{r}')\varphi_j(\boldsymbol{r})\varphi_i(\boldsymbol{r}') - \sum_{i=\beta}\sum_{j=\beta} \varphi_i^*(\boldsymbol{r})\varphi_j^*(\boldsymbol{r}')\varphi_j(\boldsymbol{r})\varphi_i(\boldsymbol{r}') \right), \tag{6}$$

where φ_j, φ_i denote occupied orbitals.

From the computational point of view, the equilibrium geometry of benzobischalcogenadiazoles and molecules structurally similar to their parts (Figure S1) was localized by Kohn-Sham method using the PBE0 functional and aug-cc-pVTZ basis set. Gaussian-09 software has been used.[S15] The attainment of the potential energy surface minima was

confirmed by the IR frequency analysis. Calculations of electron delocalization indices were carried out using AIMAll Professional.[S16] The $v_x(\boldsymbol{r})$, $v_{esp}(\boldsymbol{r})$, and $v_W(\boldsymbol{r})$ were computed using Multiwfn 3.8 [S17], while $v_x^{resp}(\boldsymbol{r})$ was calculated via our in-home program.

The found characteristics electron delocalization indices in considered compounds are given on the Fig. 2 and S1.

Table S1. The LUMO energies of the benzobischalcogenadiazoles. Electron affinity was calculated as an energy difference between neutral molecule and its anion-radical. The coefficient of determination for the dependency of the $\varepsilon_{\text{LUMO}}$ and electron affinity equals 0.98.

Compound	$\varepsilon_{\text{LUMO}}$, eV	Electron affinity, eV
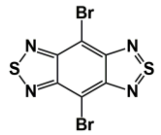	-3.896	2.587
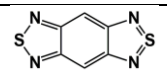	-3.604	2.174
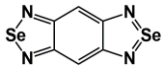	-3.788	2.389
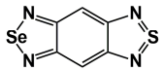	-3.697	2.283
	-3.242	2.011
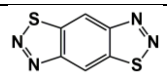	-2.919	1.577
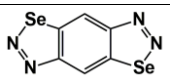	-2.896	1.635
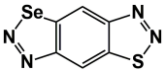	-2.902	1.603

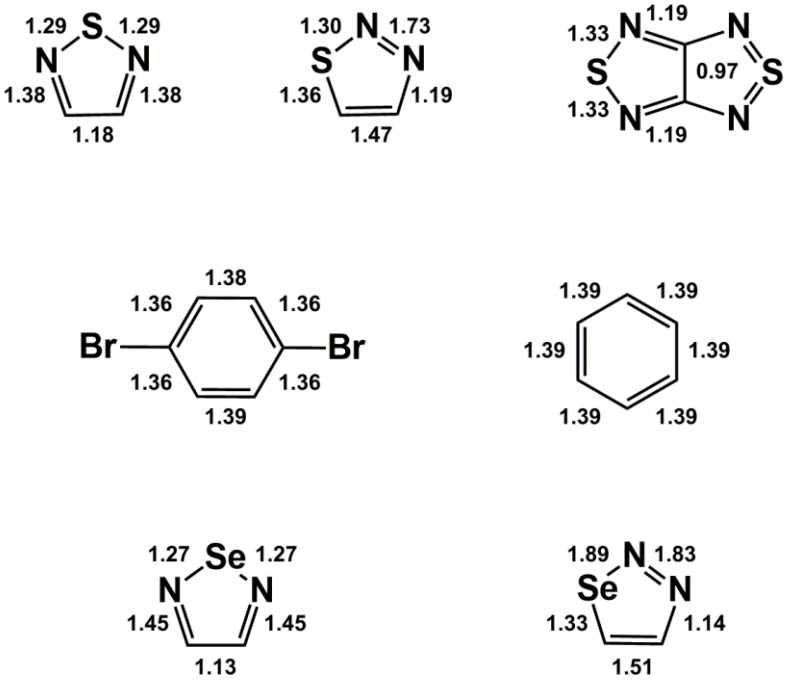

Figure S1. Delocalization indices (DI) in benzene, 1,4-dibromobenzene, 1,2,5- and 1,2,3-chalcogenadiazoles, 1,2,5-thiadiazole with two identical fused rings.

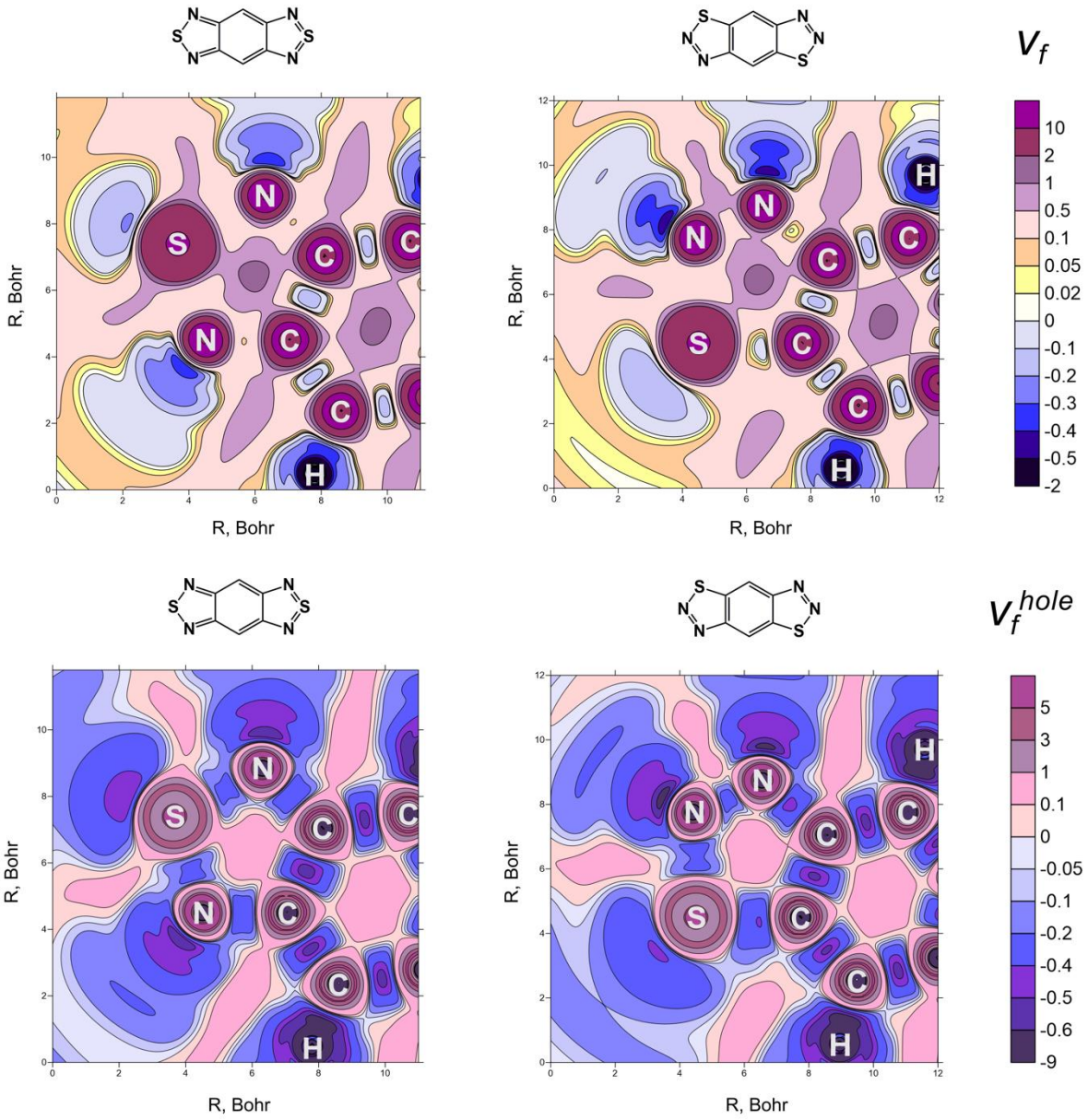

Figure S2. The distributions of the fermionic potential, $v_f(\boldsymbol{r})$, (upper panel) and its Fermi-hole dependent part, $v_f^{hole}(\boldsymbol{r}) = \int \frac{h_x(\boldsymbol{r},\boldsymbol{r}')}{|\boldsymbol{r}-\boldsymbol{r}'|} d\boldsymbol{r}' + \frac{1}{2}\int |\nabla_{\boldsymbol{r}} f(\boldsymbol{r},\boldsymbol{r}')|^2 \, d\boldsymbol{r}'$, (lower panel) in plane of the heterocyclic rings for bezobis-1,2,5- and 1,2,3-thiadiazoles. Atomic units are used.

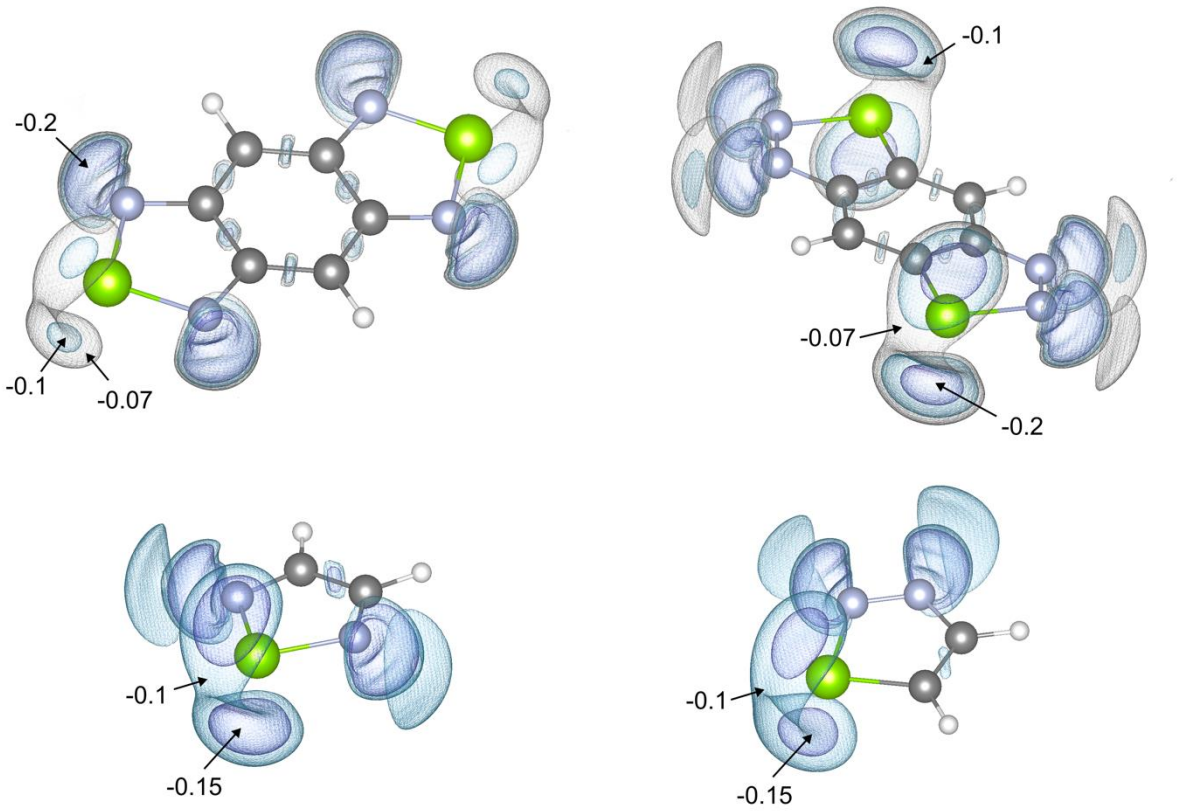

Figure S3. The 3D surfaces of the fermionic potential, v_f, for the 1,2,5- and 1,2,3-selenadiazoles and their benzobisselenadiazole analogs. The v_f values (a.u.) are explicitly given on the figure. The negative artifacts in proximity of H nucleus are not shown. C, N, Se, H atoms are shown in grey, blue, green and white correspondingly.

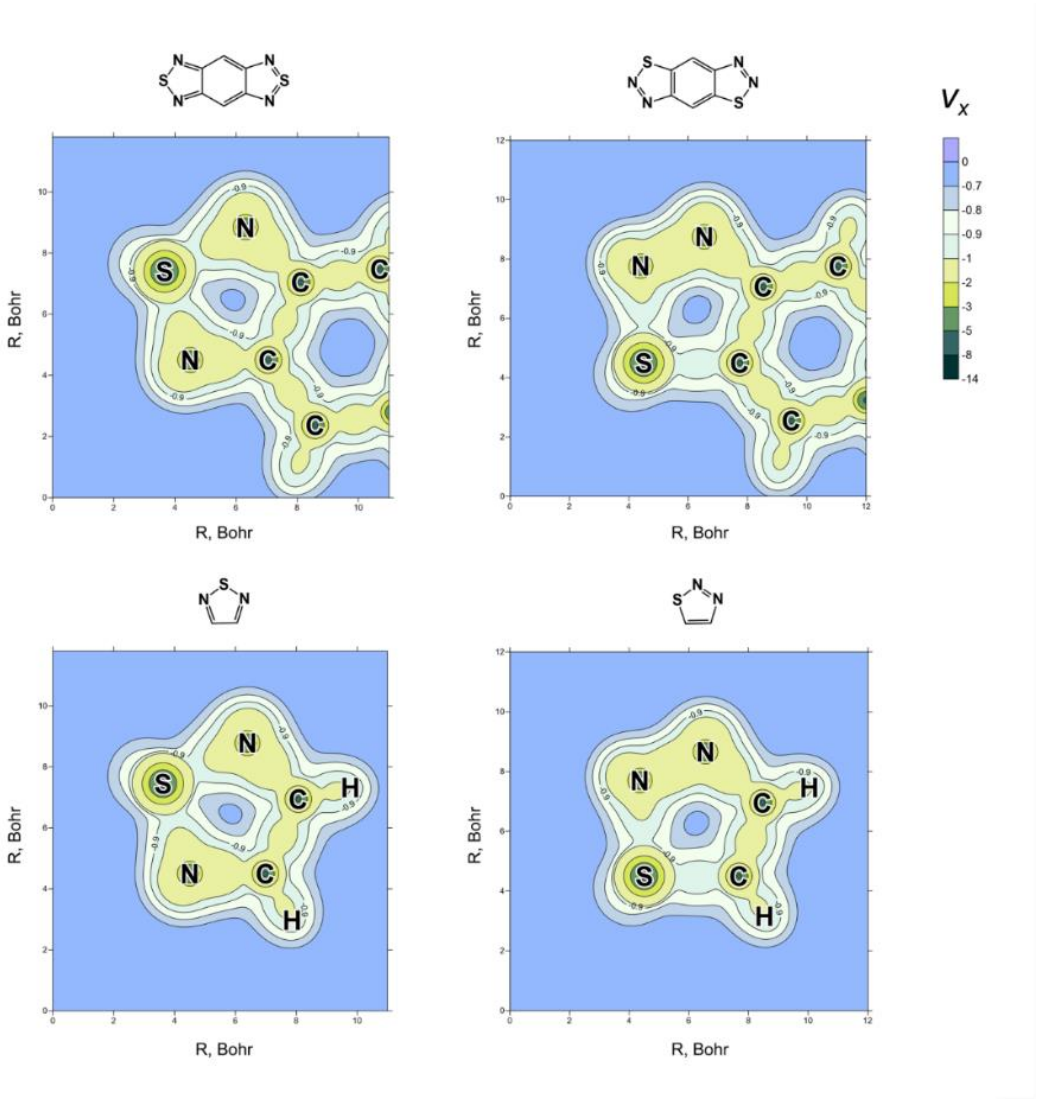

Figure S4. The distribution of the exchange potential, v_x, in plane of the heterocyclic rings for isolated 1,2,5- and 1,2,3-thiadiazoles and their analogs fused with benzene ring. Atomic units are used.

References

S1 E. O. Levina, M. G. Khrenova, A. A. Astakhov and V. G. Tsirelson, *J. Comput. Chem.*, 2022, **43**, 1000.

S2 P. R. T. Schipper, O. V. Gritsenko and E. J. Baerends, *Phys. Rev. A*, 1998, **57**, 1729.

S3 E. J. Baerends and O. V. Gritsenko, *J. Phys. Chem. A*, 1997, **101**, 5383.

S4 S. V. Kohut, A. M. Polgar and V. N. Staroverov, *Phys. Chem. Chem. Phys.*, 2016, **18**, 20938.

S5 S. Giarrusso and P. Gori-Giorgi, *J. Phys. Chem. A*, 2020, **124**, 2473.

S6 O. Gritsenko, R. van Leeuwen and E. J. Baerends, *J. Chem. Phys.*, 1994, **101**, 8955.

S7 W. L. Luken and J. C. Culberson, *Theor. Chim. Acta*, 1984, **66**, 279.

S8 Robert G. Parr and Yang Weitao, *Density-Functional Theory of Atoms and Molecules*, Oxford University Pres, Oxford, 1994.

S9 T. A. Wesolowski and Y. A. Wang, *Recent Progress in Orbital-free Density Functional Theory (vol. 6)*, World Scientific, 2013.

S10 M. Levy, J. P. Perdew and V. Sahni, *Phys. Rev. A*, 1984, **30**, 2745.

S11 V. Tsirelson and A. Stash, *Acta Crystallogr., Sect. B: Struct. Sci., Cryst. Eng. Mater.*, 2021, **77**, 467.

S12 C. Herring, *Phys. Rev. A*, 1986, **34**, 2614.

S13 S. Liu, *J. Chem. Phys.*, 2007, **126**, 244103.

S14 E. Ospadov and V. N. Staroverov, *J. Chem. Theory Comput.*, 2018, **14**, 4246.

S15 M. J. Frisch, G. W. Trucks, H. B. Schlegel, G. E. Scuseria, M. A. Robb, J. R. Cheeseman, G. Scalmani, V. Barone, B. Mennucci, G. A. Petersson, H. Nakatsuji, X. Li, H. P. Hratchian, A. F. Izmaylov, J. Bloino, G. Zheng, J. L. Sonnenberg, M. Hada, M. Ehara, K. Toyota, R. Fukuda, J. Hasegawa, M. Ishida, T. Nakajima, Y. Honda, O. Kitao, H. Nakai, T. Vreven, J. A. Montgomery, J. E. Peralta, F. Ogliaro, M. Bearpark, J. J. Heyd, E. Brothers, K. N. Kudin, V. N. Staroverov, R. Kobayashi, J. Normand, K. Raghavachari, A. Rendell, J. C. Burant, S. S. Iyengar, J. Tomasi, M. Cossi, N. Rega, J. M. Millam, M. Klene, J. E. Knox, J. B. Cross, V. Bakken, C. Adamo, J. Jaramillo, R. Gomperts, R. E. Stratmann, O. Yazyev, A. J. Austin, R. Cammi, C. Pomelli, J. W. Ochterski, R. L. Martin, K. Morokuma, V. G. Zakrzewski, G. A. Voth, P. Salvador, J. J. Dannenberg, S. Dapprich, A. D. Daniels, O. Farkas, J. B. Foresman, V. Ortiz, J. Cioslowski and D. J. Fox, 2010.

S16 AIMAll (Version 15.09.27), Todd A. Keith, TK Gristmill Software, Overland Park KS, USA, 2015 (aim.tkgristmill.com)

S17 T. Lu and F. Chen, *J. Comput. Chem.*, 2012, **33**, 580.